A Consistent Scheme for the Precise FDTD Modeling of the Graphene Interband Contribution

Stamatios Amanatiadis[1], Theodoros Zygiridis[2], Tadao Ohtani[3], Yasushi Kanai[4], and Nikolaos Kantartzis[1]

[1]Department of Electrical and Computer Engineering, Aristotle University of Thessaloniki, 54124 Thessaloniki, Greece
[2]Department of Electrical and Computer Engineering, University of Western Macedonia, 50131 Kozani, Greece
[3]Private Researcher, resides in Asahikawa 070-0841, Japan
[4]Department of Information and Electronics Engineering, Niigata Institute of Technology, Kashiwazaki 945-1195, Japan

The conductivity of graphene, due to interband electron transitions, is evaluated, in this article, as rational functions through an efficient iterative optimization of Padé polynomials. Then, the latter are straightforwardly imported in the finite-difference time-domain algorithm, as an equivalent surface current, by means of precise recursive convolution schemes. Numerical examples, considering an incident plane wave toward graphene, the extraction of the corresponding surface wave propagation attributes, and a plasmonic switch, successfully validate the consistent modeling of interband conductivity through the proposed technique.

Index Terms— **Interband conductivity, iterative optimization, Padé approximant, recursive convolution method (RCM), surface waves.**

I. Introduction

OVER a decade has, so far, elapsed since the isolation of graphene and the interest of the research community remains irreducible. This truly 2-D material presents finite conductivity despite its negligible thickness; thus, various exotic properties have been revealed, such as the ability to support surface plasmon polariton (SPP) waves. Such waves are observed at a considerably lower spectrum than conventional metals, particularly at the far and mid-infrared regime [1]. Consequently, the design of advanced devices based on graphene [2], [3] is enabled, and effective numerical algorithms are required for their trustworthy characterization.

A commendable and popular class of techniques stems from the finite-difference time-domain (FDTD) implementation that is advantageous for broadband analyses due to its explicit nature. However, it mandates specialized manipulation for the modeling of frequency-dependent media, such as graphene, where two types of electron transitions are observed, namely the intraband and interband. The former is dominant at lower spectrum, until approximately the far-infrared regime, while its frequency dependence is a Debye-like function, with various approaches reported for its accurate treatment [4], [5]. On the other hand, the latter is considered at higher frequencies and contributes in terms of a more complex conductivity function; therefore, a straightforward methodology is not feasible.

Essentially, there are two major algorithms for the modeling of graphene conductivity due to the interband contribution. Both approximate the conductivity with polynomials, imported in the FDTD method via popular schemes, such as the auxiliary differential equation (ADE) and the recursive convolution method (RCM). The first technique evaluates low-order Padé approximants and provides significant accuracy at the mid-infrared spectrum, while its performance degrades at higher frequencies [6]. The second scheme offers a satisfactory approximation at the entire spectrum, as it intuitively employs a generalized vector-fitting formulation [7], [8].

In this article, a new consistent method is developed for the precise modeling of graphene conductivity due to the interband contribution. Initially, the exact conductivity formula is studied and the correct representation of graphene as an equivalent surface current is introduced for the effective FDTD treatment [4]. Next, a detailed analysis is conducted for the appropriate functions that are optimally modeled via the RCM scheme. At first, the interband term is approximated by a direct summation of the prior functions, stressing, though, that the performance of the algorithm deteriorates seriously. Hence, several Padé approximants of $[1/2]$ order are utilized and their coefficients are optimized through an iterative process, based on key graphene parameters such as the chemical potential, which greatly minimizes the approximation error. The overall accuracy is validated via the SPP wave propagation attributes, and the transmission/reflection coefficients due to an incident plane wave toward graphene are computed. Finally, a flexible plasmonic switch is designed and thoroughly investigated.

II. Theoretical Aspects

A. Surface Conductivity of Graphene

Throughout this work, graphene is described in terms of its equivalent surface conductivity that depends on the chemical potential μ_c, scattering rate Γ, and temperature T. This conductivity is evaluated in terms of the Kubo formula as [9]

$$\begin{aligned}\sigma(\omega,\mu_c,\Gamma,T) &= \sigma_{\text{intra}}+\sigma_{\text{inter}} = \frac{e^2(j\omega+2\Gamma)}{\pi\hbar^2}\\ &\times\left[\frac{-1}{(j\omega+2\Gamma)^2}\int_0^\infty E\left(\frac{\partial f_d(E)}{\partial E}-\frac{\partial f_d(-E)}{\partial E}\right)\mathrm{d}E\right.\\ &\left.+\int_0^\infty \frac{f_d(-E)-f_d(E)}{(j\omega+2\Gamma)^2+4(E/\hbar)^2}\,\mathrm{d}E\right] \qquad (1)\end{aligned}$$

Manuscript received November 29, 2020; revised February 22, 2021; accepted March 20, 2021. Date of publication March 24, 2021; date of current version May 17, 2021. Corresponding author: N. Kantartzis (e-mail: kant@auth.gr).

Color versions of one or more figures in this article are available at https://doi.org/10.1109/TMAG.2021.3068870.

Digital Object Identifier 10.1109/TMAG.2021.3068870

where $-e$ is the electron charge, $\hbar$ is the reduced Planck's constant, $f_d(\varepsilon)$ is the Fermi–Dirac distribution, and E is the integration variable. The first term in (1) indicates the intraband contribution and is evaluated by a simple Debye-like model. Conversely, the second term, which is stronger at mid-infrared and optical frequencies, is due to interband electron transitions and is proved to be a more complex function, as summarized in [10], i.e.,

$$\sigma_{\text{inter}}(\omega) = \int_0^\infty A_E(E) \frac{j\omega + 2\Gamma}{(j\omega + 2\Gamma)^2 + 4(E/\hbar)^2} \mathrm{d}E \tag{2}$$

where $A_E(E)$ is the frequency-independent term defined as

$$A_E(E) = e^2[f_d(-E) - f_d(E)]/(\pi\hbar^2). \tag{3}$$

Moreover, the propagation characteristics of the supported SPP wave are estimated via the complex wavenumber k_ρ [10]

$$k_\rho = k_0\sqrt{1 - [2/(\sigma\eta_0)]^2} \tag{4}$$

where k_0 and η_0 are the free-space wavenumber and wave impedance, respectively. Then, the SPP wavelength, λ_{SPP}, propagation length L_{SPP} (i.e., the distance required for the SPP intensity to decay by $1/e$), and confinement ζ_{SPP}, defined as the point (perpendicular to graphene) where the wave decays to the $1/e$ of its surface value, are calculated from

$$\begin{aligned} \lambda_{\text{SPP}} &= 2\pi/\Re\{k_\rho\}, \quad L_{\text{SPP}} = -1/2\Im\{k_\rho\} \\ \zeta_{\text{SPP}} &= 1/\Re\left\{\sqrt{k_\rho^2 - k_0^2}\right\}. \end{aligned} \tag{5}$$

Finally, the reflection and transmission coefficients for a plane wave propagating toward graphene are derived via

$$R = -\sigma\eta_0/(2 + \sigma\eta_0), \quad T = 2/(2 + \sigma\eta_0). \tag{6}$$

B. RCM for the FDTD Algorithm

Graphene is plugged in the FDTD grid as surface boundary condition through the equivalent surface current $\mathbf{J}_{\text{gr}}(\mathbf{r}, \omega) = \sigma(\omega)\mathbf{E}(\mathbf{r}, \omega)$ at the xz plane, as shown in Fig. 1. Note that $\mathbf{J}_{\text{gr}}$ is computed by means of the surface conductivity and the corresponding electric field. Then, its contribution is substituted into electric-field update equations, derived from Ampere's law, as a surface current source [4]. However, the updating of the surface current is not straightforward, as the transition to the time domain necessitates a convolution

$$\mathbf{J}(\mathbf{r}, t) = \sigma(t) * \mathbf{E}(\mathbf{r}, t). \tag{7}$$

The RCM suggests that the desired convolution should be performed for a specific class of functions, including exponential and harmonic terms, in the form of

$$\sigma(t) = Ae^{-\alpha t}\cos(\omega_0 t)u(t) = \Re\{Ae^{-\gamma t}u(t)\} \tag{8a}$$

$$\sigma(t) = Ae^{-\alpha t}\sin(\omega_0 t)u(t) = \Im\{Ae^{-\gamma t}u(t)\} \tag{8b}$$

where $\gamma = \alpha - j\omega_0$ and $\Re$ and $\Im$ denote the real and imaginary parts of the function, respectively. Finally, the update equation of (7) for the specific class of functions is acquired from

$$\mathbf{J}(\mathbf{r})|^{n+\frac{1}{2}} = \Re\{Ae^{-\gamma\Delta t}\}\mathbf{J}(\mathbf{r})|^{n-\frac{1}{2}} + A\delta t\,\mathbf{E}(\mathbf{r})|^n \tag{9a}$$

$$\mathbf{J}(\mathbf{r})|^{n+\frac{1}{2}} = \Im\{Ae^{-\gamma\Delta t}\}\mathbf{J}(\mathbf{r})|^{n-\frac{1}{2}} + A\delta t\,\mathbf{E}(\mathbf{r})|^n. \tag{9b}$$

It is worth mentioning that the functions in (8) match to the popular Debye and Lorentz dispersion models. Consequently, the main objective is the time-domain (TD) representation of (2) via a combination of exponential and harmonic terms.

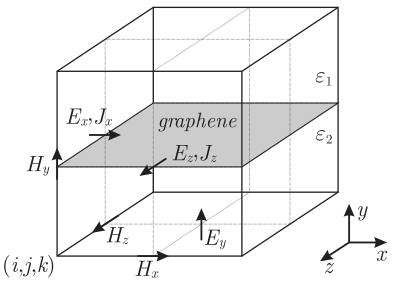

Fig. 1. Geometry of the modified Yee cell including graphene's contribution.

III. Interband Conductivity Approximation

A. Discrete Summation of Interband Conductivity

One initial approach originates from the nature of (2), since after the transition to the time domain, we derive

$$\sigma_{\text{inter}}(t) = \int_0^\infty A_E(E)e^{-2\Gamma t}\cos(2Et/\hbar)u(t)\mathrm{d}E. \tag{10}$$

The function in the integral complies with the RCM requisites, and thus, an approximation through a trapezoidal rule, which yields a discrete summation at integration points E_i, can be applied

$$\sigma_{\text{inter}}(t) = \sum_{i=0}^{N} A_E(E_i)e^{-2\Gamma t}\cos(2E_i t/\hbar)u(t)\Delta E. \tag{11}$$

Observe that N is the discrete termination of our integration to infinity and defines the number of summation terms with a maximum of $E_{\max}$. Also, ΔE is the discrete interval that approximates the infinitesimal difference between the consecutive terms. All these terms are equivalent to (8a), and the update equation of the related surface currents is given by (9a). Therefore, the total graphene contribution is launched by combining the above interband terms with the intraband one as

$$\mathbf{J}_{gr} = \sum_{i=0}^{N} \mathbf{J}_{\text{gr},i} + \mathbf{J}_{\text{gr,intra}}. \tag{12}$$

However, a detailed study indicated that a total number of over 1000 terms are required for a precise wideband approximation. Therefore, the efficiency of the FDTD algorithm is severely degraded.

B. Approximation Using Padé Polynomials

The approximation of the graphene interband conductivity with Padé polynomials has been thoroughly discussed in [6]. Nevertheless, there, a single [2/2] order polynomial was used with a seriously increasing error at higher frequencies. Thus, in this article, we propose the selection of additional Padé polynomials to minimize the approximation error, while the order is [1/2] for better compliance with RCM valid functions.

Initially, a Padé approximant of (2) is, generally, given by

$$\frac{\alpha_{0,1} + \alpha_{1,1}j\omega}{1 + \beta_{1,1}j\omega + \beta_{2,1}(j\omega)^2} = \frac{A_1(\omega)}{B_1(\omega)} \approx \sigma_{\text{inter}}(\omega). \tag{13}$$

Following [6], the calculation of the unknown coefficients, $\alpha_{0,1}$, $\alpha_{1,1}$, $\beta_{1,1}$, and $\beta_{2,1}$ requires two frequency points of the exact conductivity function. These are chosen at the limits of the spectrum, resulting in the outcomes of Fig. 2. Obviously,

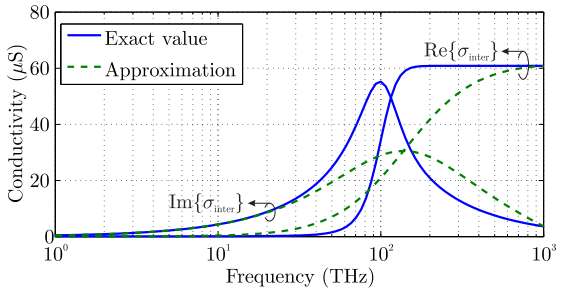

Fig. 2. Approximation of the graphene interband conductivity, with $\mu_c = 0.2$ eV and $\Gamma = 0.33$ meV, via a single Padé approximants of [1/2] order. The sampling frequencies are selected at 1 and 10^3 THz.

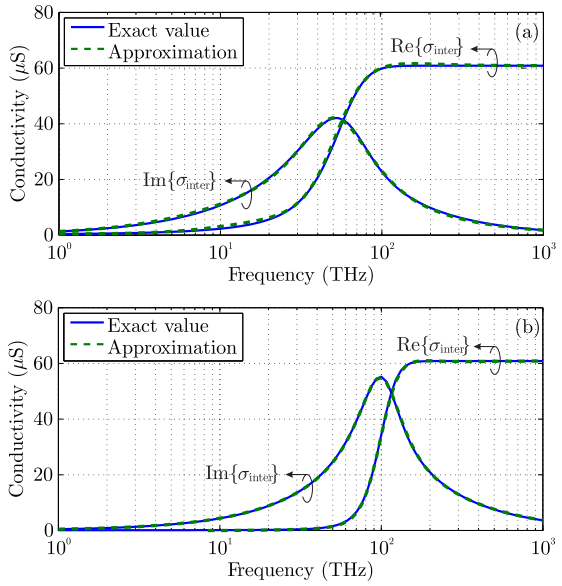

Fig. 3. Approximation of the graphene interband conductivity via two Padé approximants of [1/2] order with iteratively optimized coefficients. Graphene parameters are selected $\Gamma = 0.33$ meV and (a) $\mu_c = 0.1$ eV and (b) $\mu_c = 0.2$ eV.

the error is minimized near the exact frequency points, i.e., at the lower and upper limits of the function, and increased at the mid-range spectrum. Thus, an extra Padé approximant is employed to further annihilate the specific error, i.e.,

$$\frac{\alpha_{0,2}+\alpha_{1,2}j\omega}{1+\beta_{1,2}j\omega+\beta_{2,2}(j\omega)^2}=\frac{A_2(\omega)}{B_2(\omega)}\approx\sigma_{\text{inter}}(\omega)-\frac{A_1(\omega)}{B_1(\omega)}. \quad (14)$$

Now, the unknown coefficients are computed for frequency points selected at the mid-range spectrum, where the error maxima are actually detected. This error minimization scheme continues by adding more Padé polynomials

$$\frac{A_M(\omega)}{B_M(\omega)}\approx\sigma_{\text{inter}}(\omega)-\sum_{m=1}^{M-1}\frac{A_m(\omega)}{B_m(\omega)} \quad (15)$$

and the final interband conductivity approximation becomes

$$\sigma_{\text{inter}}(\omega)\approx\sum_{m=1}^{M}\frac{\alpha_{0,m}+\alpha_{1,m}j\omega}{1+\beta_{1,m}j\omega+\beta_{2,m}(j\omega)^2}. \quad (16)$$

C. Iterative Optimization of Padé Coefficients

In essence, the exact conductivity function is obtained at the selected frequency points of the last Padé polynomial. As the exact values of the initial ones degrade, an iterative process is proposed for optimizing the coefficients of every Padé approximant via

$$\left.\frac{A_m(\omega)}{B_m(\omega)}\right|_i\approx\sigma_{\text{inter}}(\omega)-\left.\sum_{\substack{n=1\\n\neq m}}^{N}\frac{A_n(\omega)}{B_n(\omega)}\right|_{i-1}. \quad (17)$$

The optimization occurs at a pre-processing step, so the FDTD efficiency is retained. Also, only two Padé polynomials and less than 100 iterations are actually required, as shown in Fig. 3. Here, the frequency points of the first polynomial are selected at the spectrum limits, i.e., 1 and 10^3 THz. The evaluation points for the second polynomial are chosen at the error maxima, namely at the peak of the imaginary part and near the stabilization of the real part. This is important, as the approximation is conducted through fundamental graphene parameters. In particular, the conductivity strongly depends on μ_c and the evaluation points are easily defined *a priori*.

The final step involves the TD representation of each Padé approximant to a valid form for the RCM

$$\frac{\alpha_{0,m}+\alpha_{1,m}j\omega}{1+\beta_{1,m}j\omega+\beta_{2,m}(j\omega)^2}\xrightarrow{\text{TD}}A_{p,m}\Re\{e^{-\gamma_{p,m}}u(t)\}+B_{p,m}\Im\{e^{-\gamma_{p,m}}u(t)\} \quad (18)$$

where $\gamma_{p,m}=\alpha_{p,m}-j\omega_{p,m}$ and

$$A_{p,m}=\frac{\alpha_{1,m}}{\beta_{2,m}},\qquad B_{p,m}=\frac{2\beta_{2,m}\alpha_{0,m}-\beta_{1,m}\alpha_{1,m}}{2\beta_{2,m}^2\omega_{p,m}} \quad (19a)$$

$$\alpha_{p,m}=\frac{\beta_{1,m}}{2\beta_{2,m}},\qquad \omega_{p,m}=\sqrt{\frac{4\beta_{2,m}-\beta_{1,m}^2}{4\beta_{2,m}^2}}. \quad (19b)$$

The only requirement is the real value of $\omega_{p,m}$ that leads in $4\beta_{2,m}>\beta_{1,m}^2$. If not satisfied, the harmonic term degenerates into a slow exponential decay that can be included to $\alpha_{p,m}$.

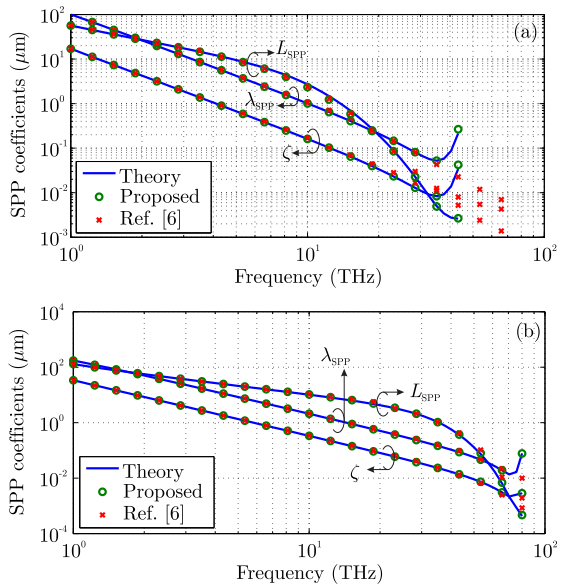

Fig. 4. Propagation characteristics of a surface wave on graphene with $\Gamma = 0.33$ meV and (a) $\mu_c = 0.1$ eV and (b) $\mu_c = 0.2$ eV.

IV. Numerical Validation

The novel methodology is validated via comparisons of numerically extracted SPP wave propagation attributes with

TABLE I
COEFFICIENTS OF (19) FOR THE APPROXIMATION OF GRAPHENE INTERBAND CONDUCTIVITY VIA TWO PADÉ POLYNOMIALS

	1st order			2nd order			
	$A_{p,1}$	$B_{p,1}$	$\alpha_{p,1}$	$A_{p,2}$	$B_{p,2}$	$\alpha_{p,2}$	$\omega_{p,2}$
$\mu_c = 0.1\,\text{eV}$	6.1×10^{-5}	-3.9×10^{8}	7.0×10^{13}	-1.0×10^{10}	-1.6×10^{10}	2.3×10^{14}	2.5×10^{14}
$\mu_c = 0.2\,\text{eV}$	6.1×10^{-5}	-2.0×10^{10}	7.0×10^{14}	-5.1×10^{9}	-2.1×10^{10}	2.6×10^{14}	5.8×10^{14}

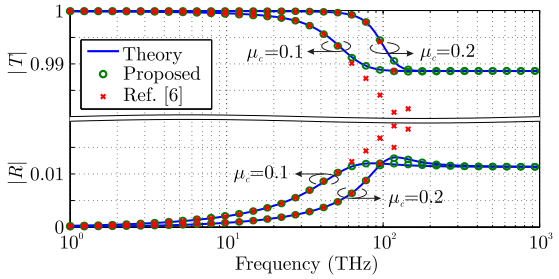

Fig. 5. Transmission and reflection for a plane wave toward graphene.

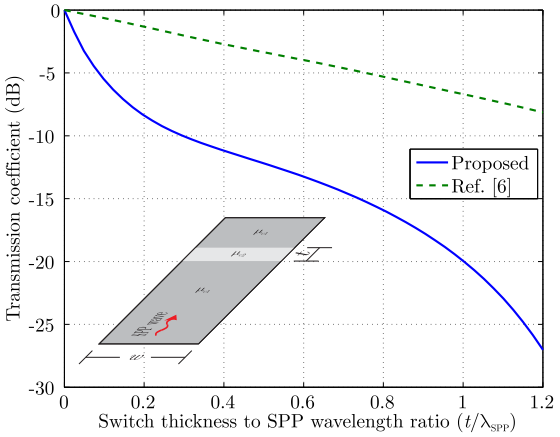

Fig. 6. Transmission coefficient at 50 THz of an SPP wave on graphene with $\mu_c = 0.2$ eV due to a switching component of $\mu_c = 0.1$ eV and thickness t.

their theoretical values, for two different sets of graphene parameters, namely we alter μ_c to 0.1 and 0.2 eV, while $\Gamma = 0.33$ meV. The interband conductivity model is approximated in Fig. 3, and the optimized coefficients are shown in Table I. Also, all simulations are conducted at the range of 1–10^2 THz since no SPP waves propagate at higher frequencies. The results of Fig. 4 indicate a remarkable agreement of our technique with the analytical values, whereas the single [2/2] Padé approximant [6] fails to accurately model the interband contribution at frequencies near the SPP wave cutoff.

The next example studies a plane wave incident upon graphene and the related reflection and transmission. The same graphene parameters and their coefficients in Table I are considered. However, in this scenario, simulations are performed at the entire frequency spectrum, i.e., 1–10^3 THz. As observed, all the outcomes of Fig. 5 prove, again, the promising approximation accuracy of the featured algorithm.

Finally, the more demanding setup of a w-wide graphene microstrip and a t-thick switching component (Fig. 6 inlet sketch) is explored. The microstrip operates at 50 THz with $\mu_{c1} = 0.2$ eV, while the switch OFF-state is attained through $\mu_{c2} = 0.1$ eV, where SPP waves are not supported [see Fig. 4(a)]. The switching effectiveness versus t is shown in Fig. 6. Evidently, a thicker switch decreases considerably the transmission due to the cutoff region of the SPP wave, thus verifying the accuracy of our method, unlike the single [2/2] Padé approximant that incorrectly permits SPP propagation.

V. CONCLUSION

The efficient modeling of graphene interband conductivity in FDTD lattices via optimized Padé approximants of [1/2] order has been introduced in this article. The new algorithm initializes the required polynomials at critical conductivity points and iteratively minimizes the approximation error. Then, the TD transition is launched in the FDTD scheme via an RCM variant. Numerical results from diverse graphene applications certified the merits of the featured method.

ACKNOWLEDGMENT

This research is co-financed by Greece and the European Union (European Social Fund- ESF) through the Operational Programme "Human Resources Development, Education and Lifelong Learning" in the context of the project "Reinforcement of Postdoctoral Researchers - 2nd Cycle" (MIS-5033021), implemented by the State Scholarships Foundation (IKY).

REFERENCES

[1] S. Xiao, X. Zhu, B.-H. Li, and N. A. Mortensen, "Graphene-plasmon polaritons: From fundamental properties to potential applications," *Frontiers Phys.*, vol. 11, no. 2, Apr. 2016, Art. no. 117801.
[2] A. Dolatabady and N. Granpayeh, "Plasmonic magnetic sensor based on graphene mounted on a magneto-optic grating," *IEEE Trans. Magn.*, vol. 54, no. 2, Feb. 2018, Art. no. 4000305.
[3] A. Hlali, Z. Houaneb, and H. Zairi, "Modeling of magnetically biased graphene coupler at THz frequency via an improved anisotropic WCIP method," *IEEE Trans. Magn.*, vol. 56, no. 8, Dec. 2020, Art. no. 2800308.
[4] G. Bouzianas, N. Kantartzis, T. Yioultsis, and T. Tsiboukis, "Consistent study of graphene structures through the direct incorporation of surface conductivity," *IEEE Trans. Magn.*, vol. 50, no. 2, Feb. 2014, Art. no. 7003804.
[5] P. C. Sarker, M. M. Rana, and A. K. Sarkar, "A simple FDTD approach for the analysis and design of graphene based optical devices," *Optik*, vol. 144, pp. 1–8, Sep. 2017.
[6] A. Mock, "Padé approximant spectral fit for FDTD simulation of graphene in the near infrared," *Opt. Mat. Exp.*, vol. 2, no. 6, pp. 771–781, 2012.
[7] H. Lin, M. F. Pantoja, L. D. Angulo, J. Alvarez, R. G. Martin, and S. G. Garcia, "FDTD modeling of graphene devices using complex conjugate dispersion material model," *IEEE Microw. Wireless Compon. Lett.*, vol. 22, no. 12, pp. 612–614, Dec. 2012.
[8] V. Nayyeri, M. Soleimani, and O. M. Ramahi, "Wideband modeling of graphene using the finite-difference time-domain method," *IEEE Trans. Antennas Propag.*, vol. 61, no. 12, pp. 6107–6114, Dec. 2013.
[9] V. Gusynin, S. Sharapov, and J. Carbotte, "Magneto-optical conductivity in graphene," *J. Phys., Cond. Matt.*, vol. 19, no. 2, pp. 1–25, 2006.
[10] G. W. Hanson, "Dyadic Green's functions and guided surface waves for a surface conductivity model of graphene," *J. Appl. Phys.*, vol. 103, no. 6, Mar. 2008, Art. no. 064302.